

First International Symposium on Microgravity Research and Applications on Physical Sciences and Biotechnology

EXPERIMENTS CONDUCTED ON COMBUSTION AT MICROGRAVITY IN THE TEXUS-38 SOUNDING ROCKET. RESULTS AND CONCLUSIONS

C. Sánchez-Tarifa
Prof. Emeritus Universidad Politécnica de Madrid
ETSIA, Plza. Cardenal Cisneros, 3. 28040 Madrid (Spain)
Tel.: +34.91.807 7171 Fax: +34.91.336 6371
E-mail: cstarifa@lmf.dmt.upm.es

B. Lázaro
SENER
Severo Ochoa, 4 (PTM). 28760 Tres Cantos (Spain).
Tel.: +34.91.807 7269 Fax: +34.91.807 7208
E-mail: benigno.lazaro@sener.es

A B S T R A C T

A series of experiments linked together on combustion at microgravity have been conducted in a TEXUS-38 sounding rocket. The experiments were performed with three cylindrical hollow rods of polymethylmethacrylate. Test were carried out in O₂-N₂ mixtures at rest and at flow velocities ranging from 10 to 30 mm/s. O₂-N₂ mixture composition changed from 40% oxygen down to pure nitrogen. The sequence of experiments consisted of: 1°.- Measurement of flame temperatures in the non-visible optical range. 2°.- Determination of O₂ concentrations at flame extinction at constant flow velocity, obtained by continuously reducing the O₂ concentration in the test section. 3°.- Measurement of flame spreading velocities. 4°.- Some information on the influence on flammability of the ignition location and time, and fuel thickness.

Main conclusions are: 1°.- Flames in the infrared, non-visible optical range have a substantially lower temperature. 2°.- O₂ concentration at flame extinction depends considerably on flow velocity, especially at low velocity levels. Final conclusion is that the flow velocity field of maximum interest is the one in which flow velocities are of the same order of magnitude as typical diffusion velocities. A follow-on program in this subject will be conducted in the US Combustion Module of the International Space Station.

1. INTRODUCTION

A research programme on the combustion of solid materials in mixtures O₂-N₂ at microgravity or reduced gravity conditions is being carried out by the Departamento de Motopropulsión y Termofluidodinámica, Escuela Técnica Superior de Ingenieros Aeronáuticos (Universidad Politécnica de Madrid).

The experimental programme has been performed in parabolic flights, utilizing the NASA KC-135 aircraft laboratory and in two sounding rockets, launched in the ESRANGE (Kiruna, Sweden) [1] [2]. The Spanish company SENER was responsible for the design and integration of the two sounding rockets tests chambers.

Lately, the research programme has been directed to the study of the basic combustion processes controlling the initiation and spread of fires in spacecraft [3] [4]. Fundamentally, these processes include flammability or ignition limits, flame spreading, and temperature and characteristics of the non visible or dim flames in the optical range that appear at microgravity at zero or at very small flow velocities under certain conditions, mainly oxygen concentration and fuel thickness. The characteristics of this type of flames are scarcely known.

This field of spacecraft fires is one of the most important applications of combustion at microgravity. In the first place, fires still remain as a major risk in spacecraft missions. According to NASA [5] five fire-causing incidents have been reported in the Space Shuttle out of a total of about 90 missions; fires that were eliminated by removal of the electric power of the circuits affected, without using fire extinguishers. On the other hand it is widely known the fire that occurred in the MIR station in 1997, which took longer than seven minutes to extinguish utilizing aqueous-foams equipment and where the crew had to wear gas masks for many hours. It is also known that several small fires have taken place in other Russian space stations.

In addition, it is being agreed that the risk of fires will increase in large and complex orbital stations, such as the International Space Station or in extraterrestrial missions that will take place in a near future.

In the second place, the knowledge of the aforementioned basic combustion processes of fires is rather incomplete, specially for thermally thick solids in the region of zero or very small convective flow velocities, where the initiation of a fire is more likely to occur. This is the case because the air currents induced in the cabins of spacecraft by the air conditioning equipment or by the motion of the crew members. According to measurements, they are of the order of a few cm/s; but in the cabin corners or in the vicinity of the walls, where the electrical cables are normally placed, the air velocities will be considerably smaller due to boundary layer effects.

2. TEXUS EXPERIMENTS

The experiments performed in the MiniTexus-3, launched from the ESRANGE (Kiruna, Sweden), in 1995 and the follow-on experiments carried out in the NASA KC-135 aircraft laboratory [2] [3] [4] were the basis for the selection of the experiments performed in the TEXUS-38 launched in the ESRANGE on April 2nd, 2000. Main purpose of these combustion experiments is the exploration of the region comprised between 0 and 30mm/s of convective flow velocity. During the six minutes at microgravity the following experiments were performed:

1. Temperature measurements and observation by IR camera at zero flow velocity of the non visible flames in the optical range. Measurements of flame temperature at 30 mm/s and 15 mm/s flow velocities of visible flames.
2. Flame spreading velocities at zero, 15 mm/s and 30 mm/s at 40% O₂.
3. Flame extinction as function of the O₂ concentrations at 30 mm/s and at 15 mm/s.
4. A limited number of experiments on the influence on the ignition process of location, time, flow velocity and rod wall thickness.

These experiments required six ignitions and a total of twelve measurements. They were performed with three cylindrical hollow rods (figure 1) placed axially in a chamber. The rods were of polymethylmethacrylate supported by a helicoidal metallic core designed to minimize the heat transferred to the rod.

In Table I the specification of all these experiments are resumed. Some of these experiments require additional remarks. The first experiment was a repetition of the one performed in the MiniTexus, but with an IR camera and moving thermocouples. However, conditions could not be exactly the same, specially the shape and volume of the chambers were different due to the space occupied by the additional diagnostics equipment. It was also known the sensitivity of the experiment regarding to producing non-visible flames. Accordingly, an alternative procedure was arranged as

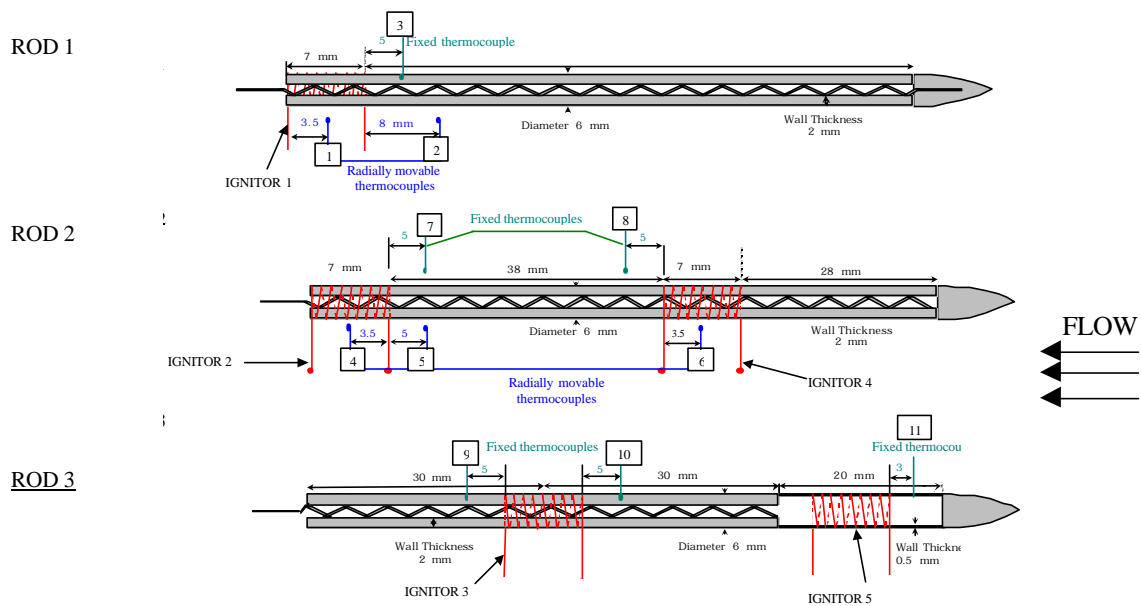


Figure 1.- Configuration of the PMMA samples used in the TEXUS-38 experiments.

shown in Table I, in which if flaming was not observed following ignition, the convective flow would be started and the ignition repeated within this flow. This was the case in the TEXUS, and, therefore, measurements of temperatures in

non-visible flames were not possible in this rod No. 1. Following ignition No. 1 bis, and after establishing an airflow of 30 mm/s, flame temperatures were measured, as well as flame spread velocity and oxygen concentration at extinction.

In rod No. 2 a similar ignition process at zero flow velocity was carried out, but with a 15 second ignition time instead of 10. In this case a non-visible flame followed ignition and it was possible to carry out temperature measurements with the radially moving thermocouples.

Ignitions were programmed at the centers of rod No. 2 (2mm thickness) and of rod No. 3 (0.5mm thickness), in order to compare the effects of location of the ignitor and thickness of the material. It was expected that ignition at the center of the rod would be considerably more difficult than ignition at the tip. The influence of the flow velocity on the ignition process was programmed for both center and tip of the rod.

No additional information is required for experiments programmed to measure flame spread velocities and O₂ concentrations for extinction.

TABLE I. TEXUS-38 EXPERIMENTS. SPECIFICATION

TABLE 1 (a)				TABLE 1 (b)			
ROD No. 1				ROD No. 1			
Experiment	O ₂ concent. and Flow Velocity	Time (experiment and total)	Remarks	ROD No. 1 Experiment	O ₂ concent. and Flow Velocity	Time (experiment and total)	Remarks
1. Ignition 1 (tip)	40% 0 mm/s	0 – 10s	If flaming does not take place: follow alternative procedure	2 Ignition 1 (tip)	40% 0 mm/s	0 – 10s	
2. Non-Visible flame. Visualisation and temp.	40% 0 mm/s	30s 40s		2' Thermocouples measurements as in the standard procedure	40% 0 mm/s	20s 30s	
3. Start convective flow and increase velocity flow up to 30 mm/s	40% 0 – 30mm/s	10s 50s		3' Start convective flow velocity	40% 0 mm/s	3s 43s	
4. Flame spread and visible flame temperature	40% 30 mm/s	25s 75s		PROCEDURE DECISION: If from all visualisations and thermocouples measurements is decided that flaming has not taken place, repeat ignition 1 as follows			
5. Reduce O ₂ concentration down to flame extinction	40% - ? 30 mm/s	20s 95s	Observe O ₂ concentration at extinction	3'' Repeat ignition 1. Flow velocity keeps increasing	40% 30mm/s	10s 53s	
6. Flush chamber with N ₂ Establish 40% O ₂ and v=0mm/s	-40% 30 – 0 mm/s	40s 135s	Small gas fluctuations might exist	4' Flame spread and visible flame temperature measurements	40% 30mm/s	22s 75s	
				5' Reduce oxygen concent. down to flame extinction	40% - ? 30mm/s	20s 95s	Observe O ₂ concentration at extinction
				6' Flush chamber with N ₂ Establish 40% O ₂ and v=0mm/s	-40% 30mm/s	40s 135s	Small gas fluctuations might exist

TABLE 1 (c)				TABLE 1 (d)			
ROD No. 2				ROD No. 3			
Experiment	O ₂ concent. and Flow Velocity	Time (experiment and total)	Remarks	Experiment	O ₂ concent. and Flow Velocity	Time (experiment and total)	Remarks
7. Ignition 2 (tip)	40% 0 mm/s	15s 150s	Small flow fluctuations might exist	13. Ignition 3 (central)	40% 15mm/s	10s 210s	Flamming may not follow ignition
8. Non-Visible flame. Visualisation and temp. measurement	40% 0 mm/s	30s 180s		14. Flame spread (downwind and upwind)	40% 15mm/s	25s 235s	
9. Set 10mm/s flow velocity. Observe flame.	40% 0 – 10mm/s	15s 195s		15. Reduce O ₂ concent. until both flames extinguish	40%? 15mm/s	25s 260s	Observe the two O ₂ concentrations when both flames extinguish
10. Increase velocity up to 15mm/s	40% 10– 15mm/s	5s 200s		16. Flush chamber with N ₂ Establish 40% O ₂ and v=0	-40% 0mm/s	40s 300s	
11. Flame spread and visible flame temp. measurements	40% - ? 15 mm/s	35s 235s		17. Ignition 4 in rod 2 (central)	40% 0mm/s	10s 310s	
12. Reduce O ₂ concent. until flame extinguishes	40% - ? 15mm/s	25s 200s	Observe O ₂ concentration at extinction	18. Ignition 5 in rod 3 (thin wall central)	40% 0mm/s	10s 320s	
				19. Observation of flames and measurements	40% 0mm/s	10-12s 320s (approx.)	

First ignition initiated 8 seconds after entering in microgravity.

3. TEST CHAMBER DESCRIPTION AND DIAGNOSTICS*

The test chamber is the third on a series of microgravity combustion rigs developed by the engineering company SENER in cooperation with Daimler-Chrysler Aerospace. A schematic view appears in Figure 2.

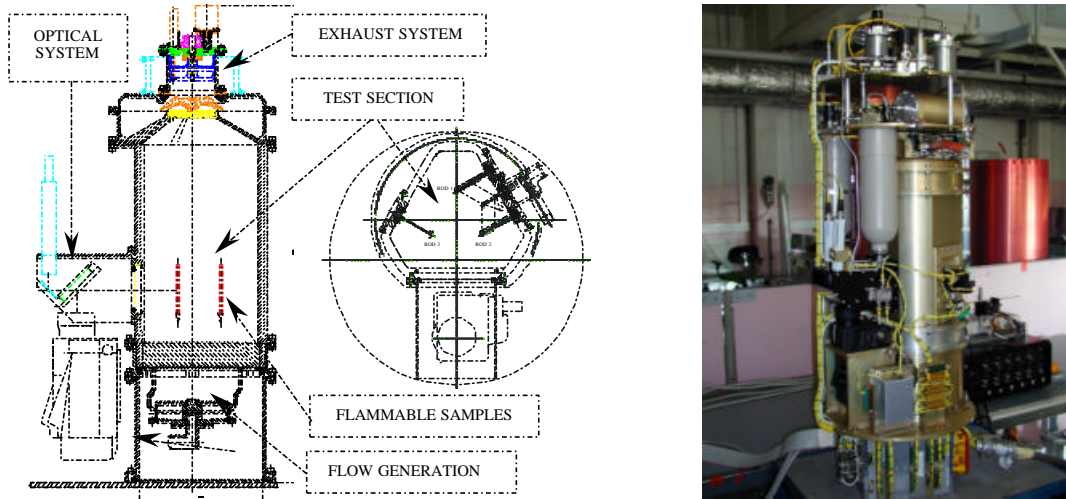


Figure 2.- Experimental chamber TEM-SEN 3. Left: Schematic lateral and plan views. Right: Built hardware before integration within the TEXUS-38 sounding rocket.

Flow is driven into the chamber from two high-pressure reservoirs containing the 40% O_2/N_2 mixture and the pure nitrogen gas. The flow rate supplied to the chamber is precisely metered through a flow regulation system and a motorized inlet needle valve working in critical conditions. The valve can be operated by telecommand and allows to continuously achieve variable test-section flow velocities in the range from 10 to 50 mm/s. Downstream from the needle valve, a flow generation system ensures that the single gas supply is transformed into a highly uniform, one-dimensional laminar flow in the test section (figure 3-a). The inlet gas and combustion products are discharged through an exhaust system, incorporating a three-stage heat exchanger and a variable area exhaust port. The pressure inside the chamber is maintained at an approximately constant level (~ 110 KPa) through an electronic unit that operates the exhaust port according to the position of the inlet needle valve. In this fashion, the test section pressure oscillations during flow transients are minimized. This characteristic proved essential when trying to obtain a well-behaved flow in the low velocity range considered.

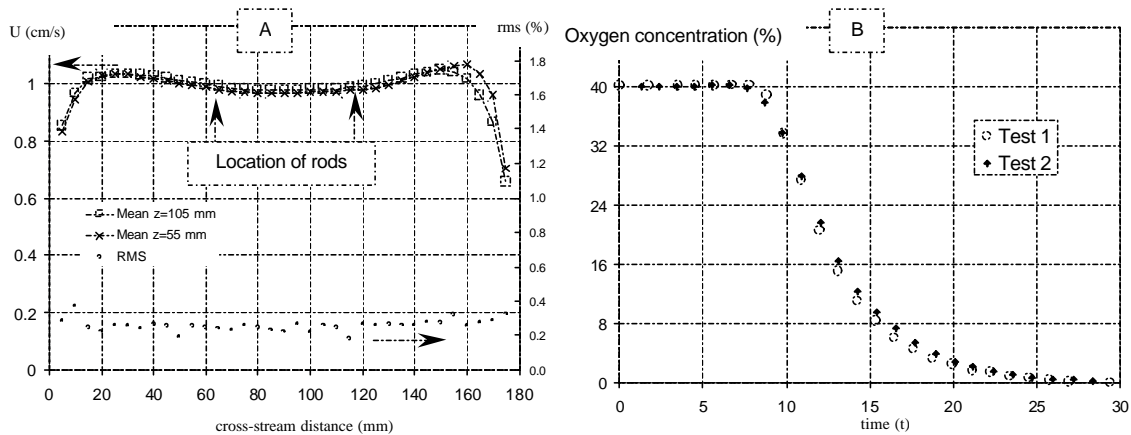


Figure 3.- A) Velocity profile obtained at the test section for the 10 mm/s flow. Measurements conducted using hot-wire anemometry. B) Oxygen concentration obtained at the location of the rods after switching the inlet supply from 40 % O_2/N_2 to pure nitrogen at $t=0$. Concentration response obtained using CO_2 as tracer and IR absorption techniques.

* Paragraphs 3 and 4 have been written with information supplied by SENER.

A compact gas mixing system is located upstream from the inlet needle valve. It consists of two reservoirs where intense mixing is achieved by using small electric fans and a two-stage, multiple-hole gas collector port. When the mixing system inlet is given a step change in the gas concentration, a smooth, continuous temporal variation of the outlet gas concentration is obtained. The characteristic time to complete the change scales with the reservoir volume and working flow rate, and is of the order of 15 s for the present design. Thus, when the mixing system inlet is exposed to a gas supply change from the 40% O₂/N₂ mixture to pure nitrogen, a O₂/N₂ gas mixture is obtained at the outlet with its oxygen contents continuously varying from 40% down to zero over a 15 s time span (figure 3-b). Ignition was carried out by electrically heating (4.5 A nominal current) 5 mm long igniters made of 0.35 mm Kantal D wire, which was wrapped around the surface of the rods. The igniters could be independently operated by telecommand. A total of 5 different ignition points were available in the present configuration. Further details of the experimental chamber can be found elsewhere [6].

For diagnostic purposes, the experimental chamber incorporated a sapphire window for infrared (IR) and visible observation. One IR as well as two visible range cameras were included for flame observation. In addition, information of the gas and solid-phase temperature field was obtained through a set of thermocouples (0.5 mm NiCr/NiAl with a 1.3 s time constant). Six of them were inserted 0.5 mm inside the rods' surface and at different axial positions. The other five were supported by a telecommand operated, motorized rake allowing a 0.55 mm/s traverse motion to obtain radial temperature profiles.

4. MEASUREMENTS

The flame visualization and the thermocouple readings were post-processed to extract information related to the flame spread velocity, the oxygen concentration at extinction, and the temperature field in the flame region. Regarding ignition, it has to be pointed out the following results:

- 1) Ignition 1 (tip, 2 mm thickness, 0 flow velocity, 10 s) did not result in flaming and, therefore, the alternative procedure had to be utilized (ignition with 30 mm/s flow velocity).
- 2) Ignition 2, similar to ignition 1 except ignition time was 15 s, resulted in flaming (upwind flame spread).
- 3) Ignition 3 (central, 2 mm thickness, 15 mm/s flow velocity, 10 s) resulted in flaming (upwind and downwind flame spread).
- 4) Ignition 4 (central, 2 mm thickness, 0 flow velocity, 10 s) resulted in no flaming as expected.
- 5) Finally, ignition 5 (central, 0.5 mm thickness, 0 flow velocity, 10 s) resulted in flaming of non-visible type.

The visible and IR visualizations of the flames obtained at different convective flow conditions are shown in Figure 4.

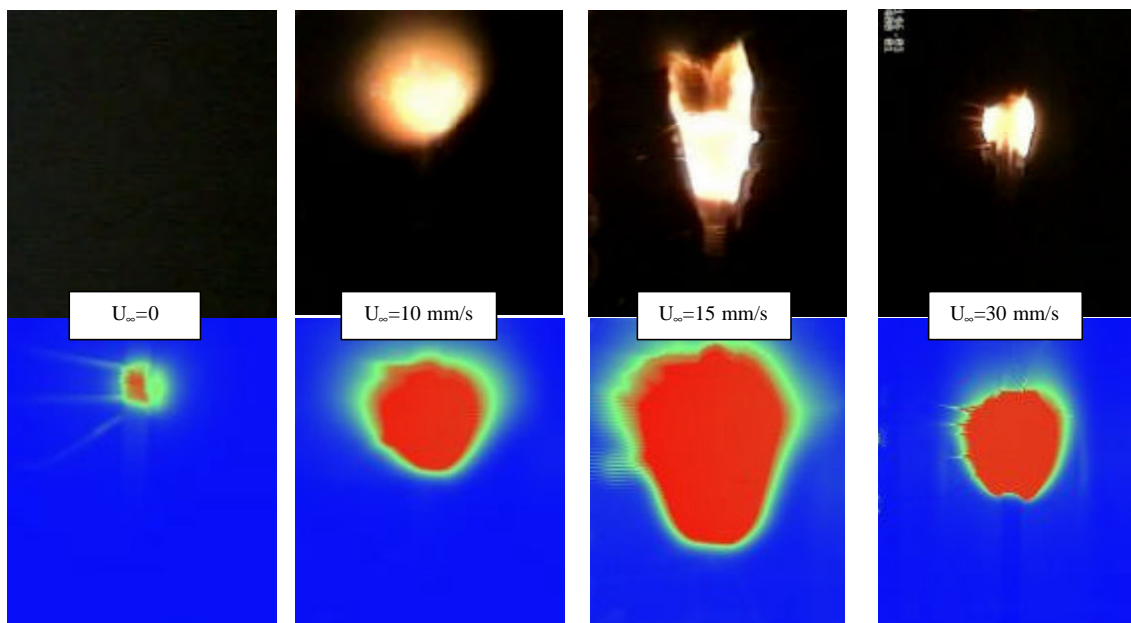


Figure 4.- Flame visualization at different flow conditions. Top: visible images. Bottom: IR images. Flow going from bottom to top of the images.

The displayed flame visualizations with no flow applied were taken 10 s after finishing ignition 2. In the visible range, the flame is almost undetectable. The IR image, however, shows a flame kernel centered at the ignition zone. The later stages of the zero flow combustion show a growing flame that becomes dim in the visible range.

Based on these data, and except for the 10 mm/s flow, flame-spreading velocities were obtained for the different flow conditions (figure 5). The available observation interval for the 10 mm/s experiment was only 10 s, insufficient to avoid transient phenomena and to provide a reliable enough measurement window.

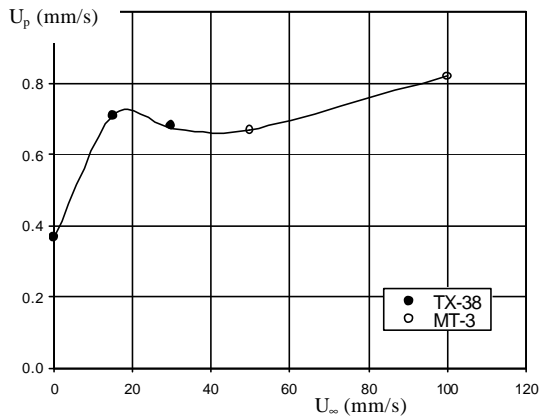


Figure 5.- Velocity of the flame front (U_p) as a function of the approaching flow velocity (U_∞). Points include measurements conducted in the present campaign (TX-38) and in a previous MiniTexus experiment (MT-3).

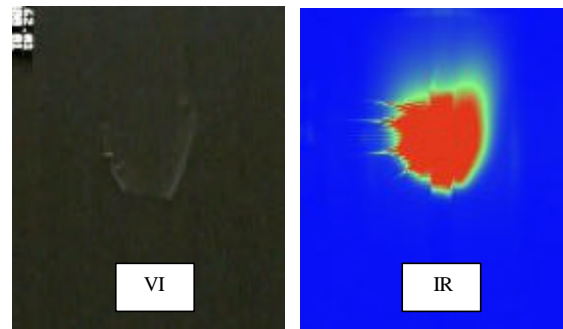


Figure 6.- Visible (VI) and infrared (IR) visualization of the flame 0.5 s prior to extinction. Approaching flow velocity is 30 mm/s. Flow going from bottom to top of the images.

The obtained flame velocities exhibit differences with respect to the behavior observed at large convective flow velocities. Specifically, the decrease in flame propagation velocity with decreasing convective flow is seen to first level in the 30 mm/s flow region, and to slightly increase at the lower 15 mm/s approaching flow speed. Finally, the flame speed decreases again when no flow is applied. The observed trends are in qualitative agreement with previous theoretical investigations [7] [8], which have identified solid-phase heat condition and radiation effects as responsible for the observed flame-spread behavior at low convection velocities.

The flame visualization obtained during the extinction process is shown in figure 6. The flame is seen to decrease its visibility as the shoot-related yellow color fades away. Just before extinction, only a thin blue reaction surface is left around the rod. It is found that, during the oxygen concentration decrease interval, no significant change occurs in the flame envelope position. Since the temporal evolution of the gas concentration within the chamber is known in advance (see figure 3), it is possible to determine the oxygen concentration when extinction takes place. This procedure gives extinction at 15% oxygen volume concentration for the 15 mm/s flow, whereas a 12% concentration characterizes the 30 mm/s extinction.

Measurements obtained with the movable thermocouple rake are presented in figure 7. The left graph shows events associated to rod 1 and ignition 1-bis. The ignition is completed at $t=57$ s. From $t=52$ to $t=70$ s, the thermocouples are located 3 mm away from the rod surface. Within this interval, the flame front reaches thermocouple T2 at $t=55$ s. As a result, the temperature shows an increase to a maximum value close to 1200 K. Following ignition ($60 < t < 65$ s), the flame front is seen to progress upstream and to collapse towards the rod. As a consequence, the distance of the flame-front to thermocouple T2 is maintained approximately constant. The measured temperature levels also exhibit constant values. During the following 5 seconds ($65 < t < 70$ s), the temperature measured by thermocouple T2 slowly decreases, as the distance from the sensor to the flame-front gradually increases. Its level is seen to approach the temperatures recorded by thermocouple T1 (~1100 K), located further downstream with respect to the flame leading edge. At time $t=70$ s the rake starts moving away from the rod surface. For thermocouple T2, the rake movement acts to maintain constant its distance to the flame-front. As a result, no significant temperature variations are measured until at $t=73$ s the extinction process is started. From there on, both T1 and T2 measured temperatures decrease. This occurs in spite of sensor T2 further approaching the flame-front. Finally, at $t=77.5$, extinction is recorded by the visible and IR flame visualizations.

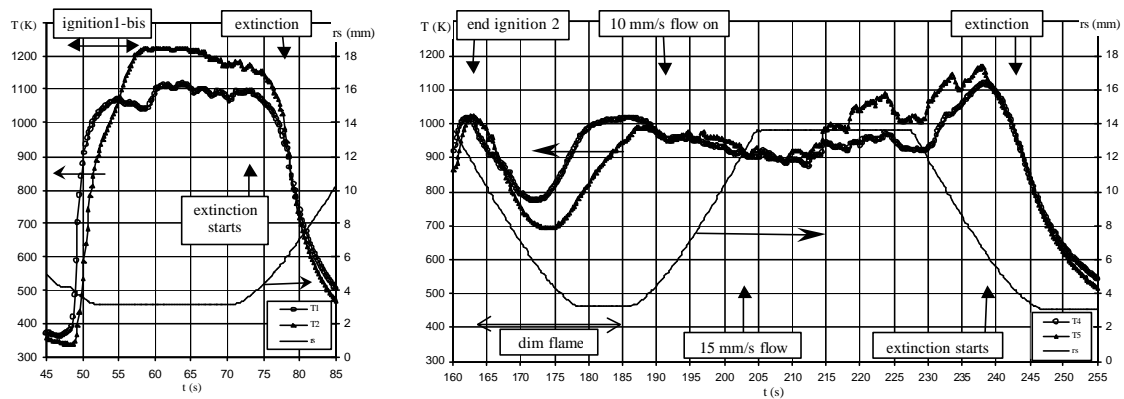


Figure 7.- Temperature temporal records obtained from the movable thermocouple rake. Left: rod 1 with 30 mm/s flow (T1, T2 thermocouples). Right: rod 2 with 0, 10 and 15 mm/s flow events (T4, T5 thermocouples). Also shown is the distance of the thermocouples to the rod surface (r_s). Time measured from the beginning of ignition 1.

The gas temperature events following ignition 2 (rod 2) are shown in the right graph of Figure 7. After switching off the igniter, the flame-front is seen to collapse towards the ignition point. It places itself at a distance that is maintained approximately constant (about 3 mm from the rod surface) during the interval $170 < t < 190$ s. In all this temporal span, the flame visibility is very low. The thermocouple rake is moved towards the rod surface in order to capture the flame temperature levels. As a result, thermocouple T4 is placed close to the flame-front for times $177 < t < 190$ s. The recorded temperature levels show an unsteady process that increases the flame-front temperature. By $t=181$ s, the recorded flame temperatures approach steady state, showing values close to 1000 K. In addition, the axial flame progression is detected by thermocouple T5, whose levels keep increasing and reach the T4 values at $t=187$ s. When the 10 mm/s flow is started ($t=191$ s), the flame-front undergoes another unsteady process, characterized by an initial expansion followed by a size decrease. At the same time, the thermocouple rake is moved outwards. This combination of events makes that, for $205 < t < 228$ s, the thermocouples are placed outside the flame and at an approximately constant distance of 5 mm. Notice also that, during this time interval, the measured temperatures levels do not exhibit significant changes. At $t=228$ s the rake is moved again towards the rod surface, thus approaching the flame front. As a result, higher temperature levels are measured. The sensors cross the flame-front at $t=238$ s, where a peak temperature of 1150 K is recorded by thermocouple T5. This value is close to the peak temperatures detected in rod 1. After $t=238$ s, the measured temperatures show a sharp decrease, which occurs as a result of the sensors leaving the flame-front region and because the extinction process has been initiated. The flame evolution during extinction is similar to that characterizing the 30mm/s experiment. Flame extinction is recorded by the visualization diagnostics at $t=242.5$ s.

5. CONCLUSIONS

Main conclusions of the present work are as follows:

- Fires still remain as an important risk in spacecraft.
- Flammability limits and flame spread velocities in solids in O_2-N_2 mixtures are the basic processes controlling the initiation and spread of fires.
- Characteristics and spread rates of the non visible flames that occur at zero or very low flow velocities should also be included as a basic process, since they might exist in the initial phases of a fire.
- The combustion region of maximum interest is the one comprised between zero flow velocity and a small velocity, somewhat higher than the values of typical diffusion velocities of the process. In this region, (0-10 or 15mm/s) the combustion regime changes drastically: combustion temperature decreases, the influence of radiation is very high, chemical kinetics has to be taken into account and the process might change from stationary to non-stationary. In addition, in this region of zero or very low flow velocities in where the initiation of fires is more likely to occur.

- The influence of small flow velocities on the combustion process is of paramount importance. Oxygen concentration at extinction may change, for example, from 15% at 15 mm/s, up to around 40% at zero flow velocity ($p \sim 100$ KPa).
- The influence of fuel thickness on flammability limits is also very important. From a limiting value of 18% of oxygen concentration for very thin fuels at microgravity [9], up to ~40% for 2mm thickness.
- Final conclusion is that further studies are very much needed on the combustion processes in the region comprised between zero and very low velocity flows. The existing information is scarce, and their knowledge would be essential for the understanding of the initiation and spread of fires in spacecraft. The large number of inter-related parameters: type of material, configuration, thickness, flow velocity, oxygen concentration and pressure, would make a test matrix very large, making the research programme specially adecuated to be carried out in a space station.

6. FOLLOW-ON PROGRAMME

As a response to NASA request: NRA-97-HEDS-01, a Proposal was submitted by the Universidad Politécnica de Madrid (UPM), to carry out a research programme in the U.S. combustion Module of the International Space Station. The Proposal: "Flame Characteristics, Flame Spread and Flammability Limits of Solids at Microgravity Conditions at Zero and at Very Small Forced Convective Flows", was written by: C.Sánchez-Tarifa, Prof. "Emeritus", UPM; A.C. Fernández-Pello, Prof. University of California (Berkeley) (at a personal basis) and M. Rodríguez, Prof. UPM.

The proposed research programme follows, in general, the lines of investigation described in the final conclusion of the preceding paragraph.

The Proposal has been approved by NASA and they have assigned, tentatively, the year 2005 to carry out the experiments. The Proposal was supported by the Plan Nacional de Investigación del Espacio, and funds are presently being requested to develop the test chamber and flow system.

7. ACKNOWLEDGMENT

The TEXUS-38 programme has been sponsored by the European Space Agency. (ESA, ESTEC Contract 12300/97/NL/CN). The Comisión de Investigación Científica y Técnica (CICYT) of Spain has supported the scientific part of the programme.

REFERENCES

- [1] C. Sánchez Tarifa, B. Lázaro and M. Rodríguez: Utilization of Sounding Rockets for Research in Microgravity Combustion. II Congreso Nacional de Ingeniería Aeronáutica, Madrid, Spain, Nov. 1993.
- [2] C. Sánchez Tarifa, J.J. Salvá and G. López Juste: Flame Spreading over Solid Fuels at Microgravity Conditions Results Obtained in the MiniTexus Rocket and Future Programmes. The First Symposium on the Utilisation of the International Space Station. 30 September – 2 October 1996, ESOC, Darmstadt, Germany.
- [3] C. Sánchez Tarifa and G. López Juste: A Study of the Combustion Problems of Solid Materials at Conditions Existing in Space Stations; Second European Symposium on Utilisation of the International Space Station, ESTEC, Noordwijk, The Netherlands, Nov. 1998.
- [4] C. Sánchez Tarifa and M. Rodríguez: Combustion and Flammability Characteristics of Solids at Microgravity in Very Small Velocity Flows. Fifth International Microgravity Combustion Workshop. NASA, Cleveland, U.S.A., May 1999.
- [5] R. Friedman, S.A. Gokoglu and L. Urban: Microgravity Combustion Research: 1999 Program and Results. NASA/TM – 1999-209198.
- [6] B. Lázaro, E. González, M. Rodríguez: Experimental Module for Weak Convection Combustion and Extinction Experiments in Microgravity Conditions. To be submitted to Experiments in Fluids, 2000.
- [7] S. Bhattacharjee, R. Altenkirch. The Effect of Surface Radiation on Flame Spread in a Quiescent Microgravity Environment. Combustion and Flame 84, 1990.
- [8] C. Sánchez-Tarifa, A. Liñán, J. Salvá, G. Lopez-Juste. Flame Spreading and Ignition on Relatively Thick Solid Fuels at Low Convective Flow Velocities and Quiescent Condition. Final Scientific Report, ESA/DASA/SENER Contracts 731/45765435 and 721/45759518, 1995.
- [9] Sandra L. Olson: NASA TM-100195, 1987.